Sign of the superexchange coupling between next-nearest neighbors in EuO

Pan Liu, Juan A.Colón Santana, Qilin Dai, Xianjie Wang, Peter A. Dowben, and Jinke Tang

Phys. Rev. B **86**, 224408 — Published 10 December 2012

DOI: 10.1103/PhysRevB.86.224408

Sign of the superexchange coupling between next nearest neighbors in EuO

Pan Liu[1], Juan A. Colón Santana[2], Qilin Dai[1], Xianjie Wang[1], Peter A. Dowben[2], and Jinke Tang[1]

[1]*Department of Physics & Astronomy, University of Wyoming, Laramie, WY 82071 USA*

[2]*Department of Physics and Astronomy and Nebraska Center for Materials and Nanoscience, University of Nebraska-Lincoln, Theodore Jorgensen Hall, 855 North 16th Street, Lincoln, Nebraska 68588-0299, USA*

ABSTRACT

The sign of the superexchange coupling J_2 between next nearest neighboring Eu^{2+} magnetic moments in EuO is a matter subject to debate. We have obtained evidence that this coupling is of antiferromagnetic nature ($J_2 < 0$). EuO thin films grown at different temperatures suggest that lattice expansion results in enhancement of T_C as clearly observed in stoichiometric EuO films grown on CaF_2 substrates. Resonant photoemission spectroscopy provides compelling evidence of strong hybridization between O 2*p* and Eu 5*d*6*s*6*p* weighted bands, suggesting that strong superexchange may be mediated by oxygen thus consistent with the observed antiferromagnetic behavior between the next nearest neighboring Eu atoms via nearest neighbor oxygen in EuO.

I. INTRODUCTION

There has been extensive research on the europium chalcogenides (EuX, X = O, S, Se, and Te) since 1961.[1] Among them, EuO has aroused more interest than many others because it is a ferromagnetic semiconductor with a higher Curie temperature (T_C) of 69 K. EuO has rock salt structure with a lattice constant of 5.144 Å and a band gap of about 1.12 eV at room temperature.[2,3] In addition, EuO has shown interesting behavior with electron doping such as a metal-to-insulator transition and colossal magnetoresistance, where the resistivity change can exceed 8-10 orders of magnitude,[4,5] much higher resistivity change than seen the famous and widely studied manganites. The Faraday rotation of EuO (~5×10^5 °/cm at 632.8 nm) is by far the highest of all known materials.[6] Recently a spin-split conduction band of about 0.6 eV in its ferromagnetic state have been shown by the studies of spin-resolved x-ray absorption spectroscopy, which creates nearly 100% spin polarized electrons close to the conduction band edge.[7] The successful integration of EuO with GaAs,[8] Si,[9-12] and GaN,[9] together with much enhanced Curie temperature via electron doping,[11-14] by pressure,[15,16] or interfacial strain,[17] makes EuO an attractive candidate for spintronic applications.

The main contributions to the magnetic coupling between Eu^{2+} spins S in EuX are the nearest neighbor (NN) exchange interaction J_1 and next nearest neighbor (NNN) exchange interaction J_2,[18-21] which are related to the T_C via the mean field expression

$$T_C = 2/3\ S(S+1)\ (12J_1 + 6J_2)/k_B. \qquad (1)$$

The indirect exchange interaction J_1 between the 12 NNs is ferromagnetic and involves a virtual transfer of a 4*f* electron to the empty 5*d* states.[22] A large positive ferromagnetic J_1 (J_1/k_B = 0.625 K as determined from single crystal inelastic neutron-scattering experiment)[19] has been widely accepted and demonstrated to be the case in a number of studies.[18-24] The superexchange interaction J_2 between the 6 NNNs may involve several mechanisms and is mostly mediated via the *p* electrons of the anions.[2] The *p* electrons of the anions polarize the 4*f* states via overlap of the anion *p* orbitals and the cation 5*d*6*s*6*p* orbitals by means of intra atomic *f*-*d* exchange. However, whether J_2 is ferromagnetic or antiferromagnetic in EuO is still a matter of

debate. Studies based on inelastic neutron-scattering on single crystals of EuO gave a positive value for J_2 (J_2/k_B = 0.125 K) and showed a ferromagnetic NNN exchange interaction,[19] consistent with the analysis on powder samples.[18] Similar results were also obtained in recent model calculations.[17,24] On the other hand, heat capacity[25,26] and NMR[27,28] measurements obtained both positive and negative J_2. Recent theoretical work using Monte Carlo calculations has suggested an antiferromagnetic NNN exchange interaction (J_2/k_B = -0.41 K) and showed that T_c decreases with the increase of the antiferromagnetic exchange coupling J_2.[16] According to Kasuya and Yanase,[29] J_2/k_B = -0.12 K. Although calculations by Wan *et al*.[24] show J_2 changes from antiferromagnetic to ferromagnetic moving from EuTe to EuO, J_2/k_B is −0.04 K for EuO with a Coulomb U of 8 eV.

The exchange interactions between local Eu^{2+} moments can be tuned by applying a hydrostatic pressure[15,16] or epitaxial strain,[17] as shown from the change in the ferromagnetic ordering temperature T_C of EuO. Hydrostatic pressure was found to increase the T_C of EuO from 69 K to above 200 K.[30,31] Utilizing epitaxial lattice strains induced in EuO or EuX films grown on substrates with smaller lattice constants, the ferromagnetic exchange interaction can increase.[17] Similar results were found when the films were sandwiched between layered materials.[32,33] The value of T_C increases when a compressive strain (shrinking of the lattice constant) is present. For tensile strain, however, there exists no clear experimental evidence showing that lattice expansion leads to decreased T_C.

In this study, we have investigated the magnetic properties of stoichiometric EuO thin films. The lattice constants were examined for stoichiometric EuO thin films grown on different substrates. When grown on CaF_2 substrates, an obvious increase in T_C was observed, which is correlated with the lattice expansion of the EuO films due to strains built during the growth. This enhancement in T_c diminishes at higher substrate temperature possibly due to strain relaxation.[34,35] We discuss the implication of such results with regard to our understanding of the magnetic coupling between neighboring Eu spins in this paper. Resonant photoemission studies give strong support for an antiferromagnetic NNN superexchange coupling hybridization

mechanism.

II. EXPERIMENTAL

For samples grown on Si substrates, the Si wafers were cleaned with dilute HF acid and rinsed with acetone, and then immediately placed in the vacuum chamber. Before the deposition, the silicon wafers were annealed at a temperature of 750º C in a chamber of pure H_2 gas of pressure 10^{-5} Torr to remove the native SiO_2 surface layer from the wafers. For samples grown on CaF_2 and MgO substrates, the substrates were cleaned with acetone, and then placed in the vacuum chamber. The CaF_2 and MgO substrates were heated to the designated deposition temperature. Pulsed laser deposition was the method used to prepare the films. The targets were Eu (99.9%) metal from Alfa Aesar, and the purity of H_2 gas used during the deposition was 99.995%. More details about the sample preparation can be found elsewhere.[11,12] To prevent the degradation of the EuO films when exposed to air, some films were protected by a Pt capping layer deposited *in situ*. The magnetic properties of stiochiometric EuO were examined using a physical properties measurement system (PPMS) from Quantum Design. X-ray diffraction (XRD) and scanning electron microscopy with energy dispersive x-ray spectroscopy (SEM-EDX) were used to investigate the films and verify they are of single phase fcc rock salt crystal structure. The lattice constants of the samples were calculated from the peak positions in the XRD patterns that are calibrated with the single crystal Si/CaF_2/MgO substrates for each measurement.

The photoemission experiments were conducted at the 3m TGM beamline[36] located at Center for Advanced Microstructures and Devices (CAMD) synchrotron at Louisiana State University.[37-39] The endstation has a 50 mm hemispherical electron energy analyzer, with a resolution of about 70 meV, as described elsewhere.[36,40] All of the photoemission spectra were taken with a 45° incidence angle and the photoelectrons were collected along the sample normal (0° emission angle). All spectra presented were normalized to the photon flux, and the secondary electron background has been subtracted. The position of the Fermi level was established

using clean Au and Cu foils as a reference. All binding energies reported here are with respect to this common Fermi level in terms of $E-E_F$, so that occupied state binding energies are negative. Energy distribution curves (EDCs) were obtained by fixing the photon energy $h\nu$ and sweeping the electron kinetic energy E_K over an energy range of about 20.0 eV within the measured Fermi level, thus measuring all the valence band common features.

III. RESULTS AND DISCUSSION

We have grown stoichiometric EuO thin films on three kinds of single crystal substrates: Si (100), MgO (100) and CaF_2 (100) to study the relationship between the lattice constant and T_C. The influence of the substrate temperature on T_C was investigated by growing EuO thin films on CaF_2 (100) single crystal substrates at different deposition temperatures (350 ℃, 400 ℃, and 500 ℃).

Figure 1 shows the XRD patterns of EuO samples on three substrates under the same grown conditions. The deposition temperature is 350℃. The stacking planes are the (200) or (111) lattice planes. The XRD peak intensities of the EuO films grown on CaF_2 (100) are much stronger than on the other two substrates, indicating the better quality and greater crystallinity of the films on CaF_2. This is probably because the crystal structure of CaF_2 is closer to EuO (both of rock salt structure) and the lattice mismatch is smaller ($a_o^{EuO} = 5.144$ Å,[2] and $a_o^{CaF2} = 5.462$ Å[41] at T = 300 K). We will focus on samples deposited on CaF_2.

The lattice mismatch between EuO and CaF_2 substrate indeed leads to a lattice expansion of the films, which can be seen from the (200) peak shift compared to the standard (dashed vertical line) and the other two films, as shown in Fig. 2. The tensile stress by the substrate results in a 0.8% lattice expansion, which is relatively large compared to other experimental data.[33] The thickness of the films ranges between 200 and 400 nm. Considering the relatively small lattice mismatch between the film and CaF_2 substrate, the critical thickness for strain relaxation should be fairly large. The known critical thickness for the onset of the relaxation for EuO films was given for films deposited on $YAlO_3$ and was found to be about 40 nm.[42] We anticipate

substantial stain be retained in our film deposited at 350℃ since it was deposited at a lower temperature, which favors greater critical thickness.[43,44] In addition, strain is generally expected in films many times thicker than the critical thickness.[44,45] EuS films 200 monolayer thick exhibits strain induced lattice expansion and contraction.[46] It is likely, on the other hand, that the induced strain gradually decreases as it is farther away from the film-substrate interface.

It is commonly expected that the T_C of EuO decreases upon lattice expansion (equivalent to a negative pressure) from various published data[16,17,31,47] and from the consideration that dominant ferromagnetic NN exchange coupling J_1 should decrease with atomic spacing. Our data show the T_C does not decrease with increased lattice constant, but instead it increases upon lattice expansion. Figure 3 shows the magnetization M as a function of temperature for the samples deposited on the three substrates (Si (100), MgO (100) and CaF_2 (100)). The Curie temperature (T_C = 71.3 K) of the EuO film grown on CaF_2 is significantly and reliably higher than the value commonly reported for EuO (T_C = 69.3 K). It is also higher than the two films deposited on Si and MgO, although the lower T_C of the latter two may be associated with the lower film quality, in addition to the absence of lattice expansion in the EuO film. In order to further investigate this phenomenon, we have deposited EuO thin films on CaF_2 (100) substrates at different deposition temperatures. Figure 4(a) shows the XRD patterns of the films grown at deposition temperatures of 350℃, 400℃, and 500℃. Higher deposition temperature leads to smaller strain in EuO, which is likely due to strain relaxation.[34,35] It was reported in Ref. [34] that dramatic softening of CaF_2 due to localized plastic flow starts at 400 ^oC. As seen in the inset of Fig. 4(a), the shift from the standard (200) peak becomes negligible for the two samples deposited at 400 and 500 ^oC, and their lattice constant decreases to that of the unstrained EuO (see Table 1). The measured values of film thickness and T_C for the various samples are also summarized in Table 1. The T_C of the two strain relaxed samples of EuO grown on CaF_2, at 400 and 500 ^oC, is 69.8 and 69.7 K, close to the expected value for EuO. The T_C was determined from Arrott-plot and inflection point of the M versus T curve, which gave consistent values for the T_C. The

magnetization as a function of temperature and its derivative dM/dT are shown in Fig. 4(b). We have also carried out experiments to study the deposition temperature dependence of Tc for EuO thin films grown on a different orientation of the CaF_2, (110). The same trend was found, that is, T_C decreases with increasing deposition temperature, which is accompanied by the decrease in lattice constant. This correlation between lattice constant and Tc was also found to hold for samples prepared with different film thicknesses.

The lattice expansion induced enhancement in T_C, discussed above, suggests antiferromagnetic coupling is at play. We believe this is, in fact, evidence for antiferromagnetic NNN exchange interaction J_2. With increasing Eu-Eu separation, this antiferromagnetic coupling plays a lesser role in preventing the overall ferromagnetic alignment of the Eu moments and, as a result, T_C increases. Although the combined ferromagnetic coupling effect of J_1 and J_2 is known to increase with compressive strains (positive pressure), there exists no reliable data showing it decreases with tensile strain (negative pressure) in a similar manner. It may well be that the lattice expansion leads to smaller magnitude for both J_1 and J_2 (J_2 at a faster pace than J_1) with the net result of an enhanced T_C. According to a high pressure x-ray absorption near edge structure (XANES) and x-ray magnetic circular dichroism (XMCD) study, although lattice contraction enhances the T_C by inducing mixing of Eu 4*f* and 5*d* electronic orbitals, a competing exchange pathway mediated by spin-polarized anion p states is predominant and counteracts the effect of the lattice contraction, limiting the T_C of EuO at ambient pressure to 70 K.[31] These experiments[31] suggest, however, the strength of this antiferromagnetic coupling does not change significantly with lattice contraction. Through their Monte Carlo calculations, Söllinger *et al*.[16] have shown a fairly sizable negative J_2, but its dependence on the lattice constant is characterized by a Grüneisen power law of exponent of about 10, slower than J_1 of exponent of 20. On the other hand, using a density functional method with explicit account for strong Coulomb repulsion within the 4*f* shell, Kuneš *et el*.[23] found nearly linear dependence of J_1 on the lattice constant, but J_2 exhibits a faster non-linear dependence. In fact, over certain values of Coulomb

potential (U = 8 eV), not only does J_2 decrease in magnitude with lattice expansion, it crosses zero and changes sign from negative to positive in EuO. Such a dependence of J_2 on the lattice constant is consistent with our observation. It should be pointed out that their calculations give mostly positive J_2 for other values of U. It should be mentioned that the increase in T_C discussed here is not related to oxygen vacancies. Oxygen-deficient EuO shows distinct double-dome shape in the M-T curve.[11-13] In addition, oxygen-deficient samples should have reduced lattice constant, which is opposite to the present case. Indeed, samples are found to be extremely resistive.

Results of resonant photoemission measurements support the presence of strong antiferromagnetic NNN superexchange interaction in EuO. A major attribute of resonant photoemission is that it allows one to distinguish which valence bands of the semiconductor host have strong rare earth 4*f* and/or simply hybridize with the Eu *4f* unoccupied continuum.[48-56] Because of the well separated oxygen weighted bands, the Eu 4*f* bands in close proximity to the Fermi level,[53,57-65] and the multiconfigurational final state features a higher binding energies,[53,65,66] Eu hybridization with the oxygen and Eu 5*d* states can be established based on the characteristics of the valence band at photoemission energies near the $4d \rightarrow 4f$ resonant photoemission condition.[53] Resonant photoemission measurements were performed on a EuO film deposited on silicon as shown in Fig. 5. Contributions from the Eu 4*f* states are evident at binding energies of -2.4 eV, followed by a strong weighted O 2*p* contribution at binding energies of 6.2 eV. In fact, Eu photoemission resonances are very common and are expected at photon energies greater than 127 eV.[53] In particular, resonances due to $4d \rightarrow 4f$ excitations are expected at photon energies of about 140.5 eV, as seen in Fig. 6 for the Eu 4*f* weighted valence band feature at about -2 eV binding energy. This process can be described as

$$4d^{10}4f^{7}+h\nu \rightarrow 4d^{10}4f^{6}+e^{-} \qquad (2)$$

$$4d^{10}4f^{7}+h\nu \rightarrow 4d^{9}4f^{8} \rightarrow 4d^{10}4f^{6}+e^{-} \qquad (3)$$

where (2) is a direct photoionization process and (3) is a super Coster-Kronig transition process. In fact not only do the Eu weighted valence band features show a

resonant enhancement with photon energies near the Eu 4d core level, the oxygen weighted valence band features also exhibit a strong resonance as well.

Neglecting the oxygen k-shell, all oxygen resonances are expected to occur at small photon energies. However, the enhancement in the photoemission intensity for the valence band feature located around 6.0 eV binding energy, as one probes the Eu resonance in the region of an incident photon energy of about 140 to 150 eV, is also seen to occur. These resonances occur at photon energies somewhat higher (145 eV photon energy) than those (140 eV photon energy) corresponding to (3). In fact excitations of the form

$$\begin{aligned} &\mathrm{Eu}[4d^{10}4f^{7}(5d6s6p)^{2}]\mathrm{O}[2p^{4}]+h\nu \rightarrow \mathrm{Eu}[4d^{9}4f^{7}(5d6s6p)^{3}]\mathrm{O}[2p^{4}] \\ &\rightarrow \mathrm{Eu}[4d^{10}4f^{7}(5d6s6p)^{2}]\mathrm{O}[2p^{3}]+e^{-} \end{aligned} \quad (4)$$

are also possible[53,66] and could contribute to a Fano-resonance with

$$\mathrm{Eu}[4d^{10}4f^{7}(5d6s6p)^{2}]\mathrm{O}[2p^{4}]+h\nu \rightarrow \mathrm{Eu}[4d^{10}4f^{7}(5d6s6p)^{2}]\mathrm{O}[2p^{3}]+e^{-} \quad (5)$$

but would only contribute the oxygen weighted valence band feature if there existed strong hybridization between 2*p* oxygen band and Eu 5*d*6*s*6*p* weighted bands, so that a final state of Eu[$4d^{10}4f^{7}(5d6s6p)^{2}$]O[$2p^{3}$] becomes possible, even with the initial excitation on the Eu site. This is compelling evidence of Eu and O hybridization involving some of the unoccupied Eu *4f* levels. This hybridization between Eu and O in turn could play a significant role in the NNN superexchange coupling seen in the EuO films. In fact these hybrid bands would be expected to be significantly more itinerant than the 4*f* weighted bands and are essential to the superexchange coupling mediated by the overlap of the oxygen 2*p* orbitals and the Eu 5*d*6*s*6*p* orbitals via intra atomic *f-d* exchange.

The resonance of the multiconfigurational final states that give rise to the valence band photoemission features at about 9 eV binding energy is the result of the additional energy cost associated with excitations to the $4f^{7}(5d6s6p)^{3}$ hybridized band, similar to the photon energy dependent resonances associated with the oxygen weighted states seen in the valence band photoemission spectra. But it also suggests that there is Eu *4f-5d-6s* hybridization as well.

It should be mentioned here that the existence of strong hybridization between O 2*p* and Eu 5*d*6*s*6*p* weighted bands seen in EuO should not be dependent on the substrate (Si, MgO or CaF_2). Only the degree of such hybridization may be changed by the choice of the substrates. We would like to note, in addition, that in rare earth metals like Gd,[67,68] T_C will also increase with an increasing lattice constant because of an increased intraatomic 5*d*4*f* overlap due to the increased 5*d* localization, leading to an increase in the polarization of the itinerant electrons even as J_1 decreases.[68,69] With EuO, the nominally 2+ valence makes this mechanism inappropriate as this is a semiconductor and not a metal.

V. CONCLUSIONS

Antiferromagnetic NNN exchange coupling J_2 is suggested as a result of the investigation of stoichiometric EuO grown on CaF_2 at various temperatures. Tensile strain induced in the films leads to an observable enhancement in T_C from 69.7 to 71.3 K. Resonant photoemission provides evidence of strong hybridization between the Eu and oxygen so that the unoccupied bands of Eu 5*d*6*s*6*p* character must also contain significant O 2*p* weight as well. These results combined provide strong support for the antiferromagnetic NNN superexchange coupling.

ACKNOWLEDGEMENTS

This work was supported by the National Science Foundation (DMR-0852862 and CBET-0754821), the U.S. Department of Energy, Office of Basic Energy Sciences, Division of Materials Sciences and Engineering under Award DE-FG02-10ER46728, the Nebraska Materials Science and Engineering Center DMR-0820521) and the Defense Threat Reduction Agency (DTRA) through Grant No. HDTRA1-07-1-0008.

REFERENCES

[1]B. T. Matthisa, R. M. Bozorth, and J. H. Van Vleck, Phys. Rev. Lett. **7**, 160 (1961).

[2]A. Mauger and C. Godart, Phys. Rep. **141** 51(1986).

[3]N.Tsuda, K. Nasu, A. Fujimori, and K. Siratori, Electronic Conduction in Oxides, Springer Series in Solid-State Sciences (Springer, New York, 2000).

[4]M. R. Oliver, J. O. Dimmock, A. L. McWhorter, and T. B. Reed, Phys. Rev. B **5** 1078 (1972).

[5]Y.Shapira, S. Foner, R. L. Aggarwal, and T. B. Teed. Phys. Rev. B **8** 2316 (1973).

[6]K.Y. Ahn and J.C. Suits, IEEE Trans. Magn. MAG-**3**, 453 (1967).

[7]P.G. Steeneken, L.H. Tjeng, I. Elfimov, G.A. Sawatzky, G. Ghiringhelli, N.B. Briikes, and D.J. Huang, Phys. Rev. Lett. **88** 047201 (2002).

[8]A. G. Swartz, J. Ciraldo, J. J. I. Wong, Y. Li, W. Han, T. Lin, S. Mack, J. Shi, D. D. Awschalom, and R. K. Kawakami, Appl. Phys. Lett. **97**, 112509 (2010).

[9]A. Schmehl, V. Vaithyanathan, A. Herrnberger, S. Thiel, C. Richter, M. Liberati, T. Heeg, M. Röckerath, L.F. Kourkoutis, S. Mühlbauer, P. Böni, D. A. Muller, Y. Barash, J. Schubert, Y. Idzerda, J. Mannhart, and D. G. Schlom, Nature Mater. **6** 882 (2007).

[10]R. P. Panguluri, T. S. Santos, E. Negusse, J. Dvorak, Y. Idzerda, J. S. Moodera, and B. Nadgorny, Phys. Rev. B **78**, 125307 (2008).

[11]X. Wang, P. Liu, K. A. Fox, J. Tang, J. Colón Santana, K. Belashchenko, P. Dowben, and Y. Sui, IEEE Tran. On Mag. **46** 6 (2010).

[12]P. Liu, J. Tang, J. Colón Santana, K. D. Belashchenko, and P. Dowben, J. Appl. Phys. **109**, 07C311 (2011).

[13]T. Matsumoto, K. Yamaguchi, M. Yuri, K. Kawaguchi, N. Koshizaki, and K. Yamada. J. Phys. Condens. Matter **16** 6017 (2004).

[14]T. Mairoser, A. Schmehl, A. Melville, T. Heeg, W. Zander, J. Schubert, D. E. Shai, E. J. Monkman, K. M. Shen, T. Z. Regier, D. G. Schlom, and J. Mannhart, Appl. Phys. Lett. **98**, 102110 (2011).

[15]V. G. Tissen and E. G. Ponyatovskii, JETP Lett. **46**, 361 (1988).

[16]W. Söllinger, W. Heiss, R. T. Lechner, K. Rumpf, P. Granitzer, H. Krenn, and G. Spingholz, Phys. Rev. B **81**, 155213 (2010).

[17]N. J. C. Ingle and I. S. Elfimov, Phys. Rev. B **77**, 121202 (R) (2008).

[18]L. Passell, O. W. Dietrich, and J. Als-Nielsen, Phys. Rev. B **14**, 4897 (1976).

[19]H. A. Mook, Phys. Rev. Lett. **46**, 508 (1981).

[20]V. C. Lee and L. Liu, Phys. Rev. B **30**, 2026 (1984).

[21]I. N. Goncharenko and I. Mirebeau, Phys. Rev. Lett. **80**, 1082 (1998).

[22]J. B. Goodenough, J. Appl. Phys. **34**, 1193 (1963).

[23]J. Kunes, W. Ku, and W. E. Pickett, J. Phys. Soc. Jpn. **74**, 1408 (2005).

[24]X. Wan, J. Dong, and S. Y. Savrasov, Phys. Rev. B **83**, 205201 (2011).

[25]A. J. Henderson, G. R. Brown, T. B. Reed, and H. Meyer, J. Appl. Phys. **41**, 946 (1970).

[26]O.W. Dietrich, A. J. Henderson, and H. Meyer, Phys. Rev. B **12**, 2844 (1975).

[27]E. L. Boyd, Phys. Rev. **145**, 174 (1966).

[28]A. Comment, J.-P. Ansermet, C. P. Slichter, H. Rho, C. S. Snow, and S. L. Cooper, Phys. Rev. B **72**, 014428 (2005).

[29]T. Kasuya and A. Yanase, Rev. Mod. Phys. **40**, 684 (1968).

[30]M. M. Abd-Elmeguid and R. D. Taylor, Phys. Rev. B **42**, 1048 (1990).

[31]N. M. Souza-Neto, D. Haskel, Y. C. Tseng, and G. Lapertot, Phys. Rev. Lett. **102**, 057206 (2009).

[32]A. Stachow-Wójcik, T. Story, W. Dobrowolski, M. Arciszewska, R. R. Gała□zka, M. W. Kreijveld, C. H. W. Swüste, H. J. M. Swagten, W. J. M. de Jonge, A. Twardowski, and A. Yu. Sipatov, Phys. Rev. B **60** 15220 (1999).

[33]R. T. Lechner, G. Springholz, T. U. Schülli, J. Schwarzl, and G. Bauer, Phys. Rev. Lett. **94**, 157201 (2005).

[34]N. P. Skvortsova, E. A. Krivandina, and D. N. Karimov, Phys. Solid. Stat. **50** 665 (2008).

[35]H. Ogino, N. Miyazaki, T. Mabuchi, and T. Nawata, J. Crystal Growth, **310** 221 (2008).

[36]Y. Losovyj, I. Ketsman, E. Morikawa, Z. Wang, J. Tang, P. A. Dowben, Nucl. Instrum. Methods Phys. Res. A **582**, 264 (2007).

[37]J. Hormes, J. D. Scott, V. P. Suller, Synchrotron Radiation News **19**, 27 (2006).

[38]A. Roy, E. Morikawa, H. Bellamy, C. Kumar, J. Goettert, V. Suller, K. Morris, D. Ederer, J. Scott, Nuc. Instrum. Methods Phys. Res. A **582**, 22-25 (2007).

[39]E. Morikawa, J. D. Scott, J. Goettert, G. Aigeldinger, C. S. S. R. Kumar, B. C. Craft, P. T. Sprunger, R. C. Tittsworth, F. J. Hormes, Rev. Sci. Instrum. **73**, 1680-1683 (2002).

[40]P. A. Dowben, D. LaGraffe, M. Onellion, J. Phys. Cond. Matter **1**, 6571 (1989).

[41]J. P. Stott, B. A. Bellamy, L. W. Hobbs, W. Hayes, A. E. Hughes, J. Phys. C: Solid State Phys. **9**, L223 (1976).

[42]R. W. Ulbricht, A. Schmehl, T. Heeg, J. Schubert, D. G. Schlom, Appl. Phys. Lett., **93**, 102105 (2008).

[43]B. J. Spencer, P. W. Voorhees, and S. H. Davis, Phys. Rev. Lett., **67**, 3696 (1991).

[44]B.W. Dodson and J.Y. Tsao, Appl. Phys. Lett, **51**, 1325 (1987).

[45]D. J. Dunstan, S. Young, and F.L.H. Dixon, J. Appl. Phys., **70**, 3038 (1991).

[46]A. Stachow-Wójcik, T. Story, W. Dobrowolski, M. Arciszewska, R. R. Galązka, M. W. Kreijveld, C. H. W. Swüste, H. J. M. Swagten, W. J. M. de Jonge, A. Twardowski, and A. Yu. Sipatov, Phys. Rev. B, **60**, 15220 (1999).

[47]K. Lee and J.C. Suits, J. Appl. Phys., **41**, 954 (1970).

[48]J. Shi, M. V. S. Chandrashekhar, J. Reiherzer, W. Schaff, J. Lu, F. Disalvo and M. G. Spencer, Phys. Status Solidi C **5**, 1495 (2008).

[49]T. Thomas, X. M. Guo, M. V. S. Chandrashekhar, C. B. Poitras, W. Shaff, M. Dreibelbis, J. Reiherzer, K. W. Li, F. J. DiSalvo, M. Lipson, and M. G. Spencer, J. Cryst. Growth, **311**, 4402-4407 (2009).

[50]A. J. Steckl, J. H. Park, and J. M. Zavada, Mater. Today **10**, 20 (2007).

[51]G. H. Dieke and H. M. Crosswhite, Appl. Optics **2**, 675-686 (1963).

[52]S. R. McHale, J. W. McClory, J. C. Petrosky, J. Wu, R. Palai, Ya. B. Losovyj, and P. A. Dowben, European Physical Journal: Applied Physics **56**, 11301 (2011).

[53]J.A. Colón Santana, Pan Liu, X. Wang, J. Tang. S.R. McHale, D. Wooten, J.W. McClory, J.C. Petrosky, J. Wu, R. Palai, Ya. B. Losovjy, and P.A. Dowben, J. Physics: Cond. Matt. **24**, 445801 (2012).

[54]G. J. Lapeyre, J. Anderson, P. L. Gobby, and J. A. Knapp, Phys. Rev. Lett. **33**, 1290 (1977).

[55]I. Ketsman, Ya. B. Losovyj, A. Sokolov, J. Tang, Z. Wang, K. D. Belashchenko and P.A. Dowben, Appl. Phys. A: Mater. Sci. Process. **89**, 489 (2007).

[56]L. Wang, W.-N. Mei, S. R. McHale, J. W. McClory, J. C. Petrosky, J. Wu, R. Palai, Ya. B. Losovyj, and P. A. Dowben, *Semiconductor Science and Technology* **27**, 115017 (2012).

[57]J. Kunes, W. Ku, and W. P. Pickett, J. Phys. Soc. Jpn. **74**, 1408 (2005).

[58]D. B. Ghosh, M. De, and S. K. De, Phys. Rev. B **70**, 115211 (2004).

[59]N. J. C. Ingle and I. S. Elfimov, Phys. Rev. B **77**, 121202(R) (2008).

[60]R. Schiller, O. Myrasov, A. J. Freeman, and W. Nolting, J. Magn. Magn. Mater. **226**, 388 (2001).

[61]H. Miyazaki, T. Ito, H. J. Im, S. Yagi, M. Kato, K. Soda, and S. Kimura, Phys. Rev. Lett. **102**, 227203 (2009).

[62]H. Miyazaki, T. Ito, S. Ota, H. J. Im, S. Yagi, M. Kato, K. Soda, and S.-I. Kimura, Physica B **403**, 917 (2008).

[63]P. Munz, Helv. Phys. Acta **49**, 281 (1976).

[64]D. E. Eastman, F. Holtzberg, and S. Methfessel, Phys. Rev. Lett. **23**, 226 (1969).

[65]J. A. Col´on Santana, J. M. An, N. Wu, K. D. Belashchenko, X. Wang, P. Liu, J. Tang, Ya. Losovyj, I. N. Yakovkin, P. A. Dowben, Phys. Rev. B **85**, 014406 (2012)

[66]W. D. Schneider, C. Laubschat, G. Kalkowski, J. Haase, A. Puschmann, Phys. Rev. B **28**, 2017 (1983).

[67]C. Waldfried, T. McAvoy, D. Welipitiya, P.A. Dowben, and E. Vescovo, *EuroPhysics Letters* **42**, 685 (1998).

[68]T. Komesu, C. Waldfried and P.A. Dowben, *Phys. Lett.* A **256**, 81 (1999).

[69]T. Komesu, H. K. Jeong, David Wooten, Ya. B. Losovyj, J. N. Crain, M. Bissen, F. J. Himpsel, J. Petrosky, J. Tang, W. Wang, I.N. Yakovkin, and P. A. Dowben, *Physica Status Solidi* B **246**, 975 (2009).

Table 1. Comparison of lattice constant, Curie temperature and film thickness for EuO films grown on CaF_2 (100) at different deposition temperatures

	CaF_2 (100)		
Substrate temperature (℃)	350	400	500
Lattice constants (nm)	0.5181	0.5145	0.5138
Curie temperature (K)	71.3	69.8	69.7
Film thickness (nm)	420	360	240

Figure Captions

Figure 1 XRD patterns of EuO thin films grown on Si (100), MgO (100) and CaF_2 (100) substrates.

Figure 2 Enlarged views of XRD patterns around the EuO (200) peaks for three substrates. The doted vertical line is the position of the standard EuO (200) peak.

Figure 3 Magnetizations as a function of temperature for EuO thin films grown on three substrates.

Figure 4 (a) XRD patterns of EuO thin films grown on CaF_2 (100) substrates at different deposition temperatures; the inset shows enlarged view of XRD patterns about the EuO (200) peaks. (b) Magnetizations as a function of temperature for EuO thin films grown at different deposition temperatures on CaF_2 (100) substrates; inset shows the derivative of the magnetization as a function of temperature.

Figure 5 Resonant photoemission spectra obtained for the EuO films on Si (100). The photon energy ranges from 125 eV (bottom) to 165 eV (top). Resonant enhancements observed at a binding energy of -2.4 eV correspond to constructive interference between a direct 4*f* photoionization and a super Coster-Kronig transition as described in the text. Electrons were collected normal to the surface at a temperature of 100 ^{0}C to eliminate residual charging effects.

Figure 6 Resonance line shape as extracted from the constant initial state valence data for the EuO on Si (100) films. These features correspond to (a) Eu $4f^6$ (-2.4 eV binding energy), (b) O 2*p* (-6 eV binding energy) and (c) Eu $4f^5$ (-9 eV binding energy).

Figure 1

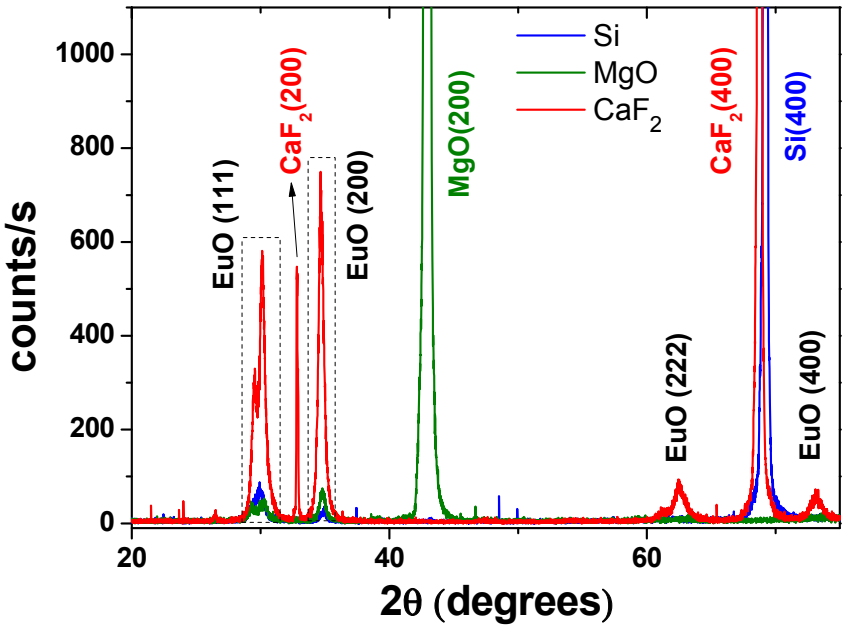

Figure 2

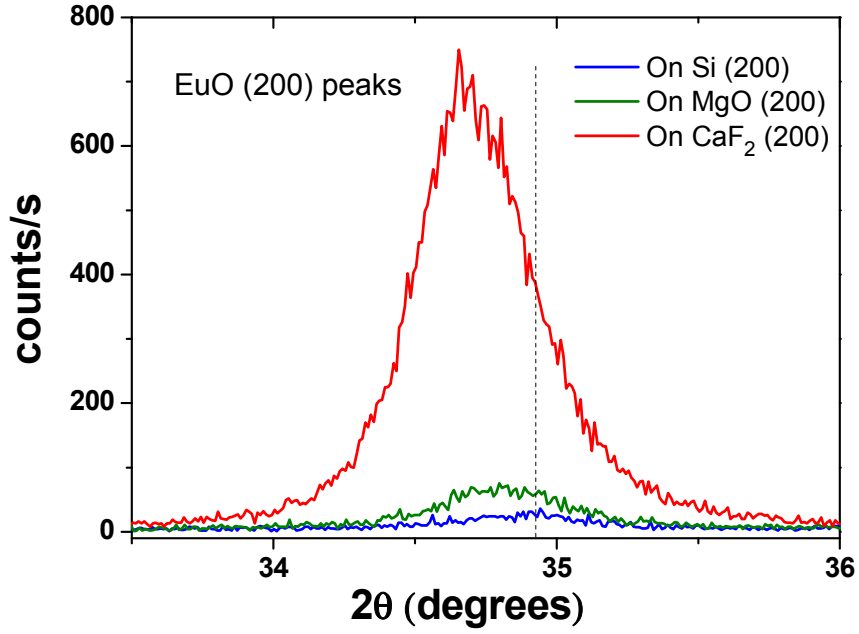

Figure 3

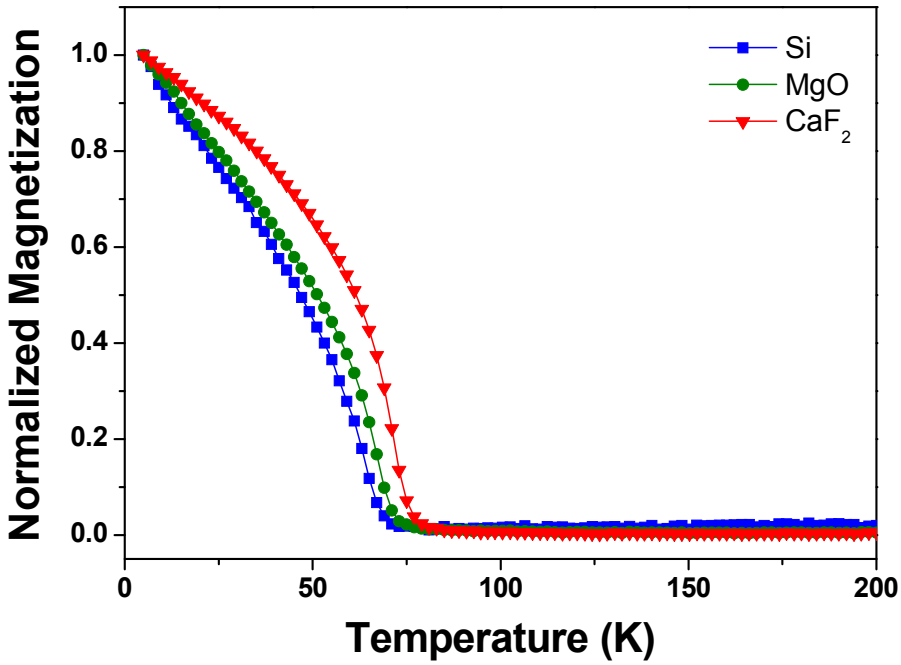
Normalized Magnetization
1.0
0.8
0.6
0.4
0.2
0.0
0
50
100
150
200
Temperature (K)
Si
MgO
CaF2

Figure 4

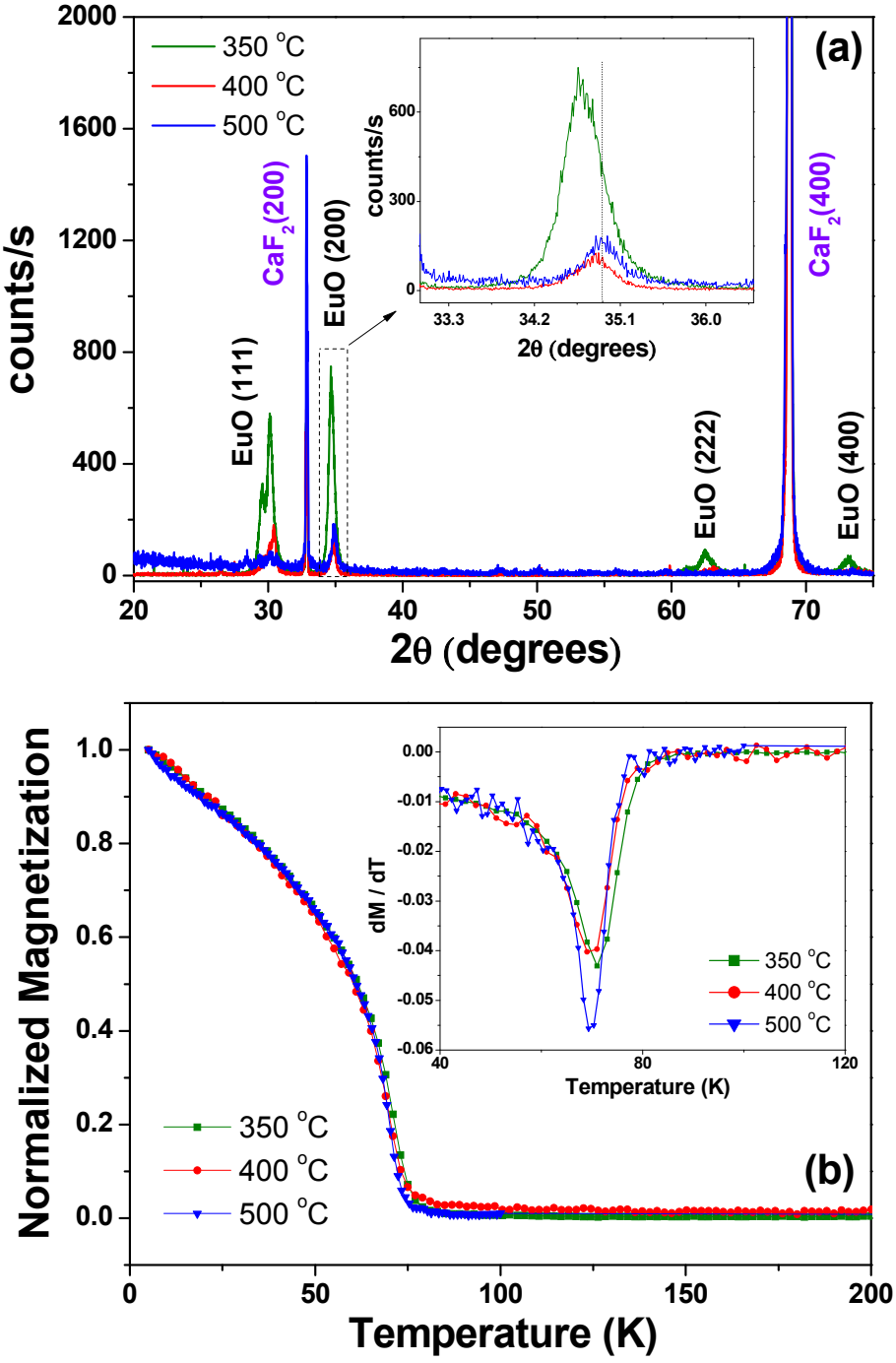
(a)
350 °C
400 °C
500 °C
counts/s
2θ (degrees)
EuO (111)
CaF2(200)
EuO (200)
EuO (222)
CaF2(400)
EuO (400)
(b)
Normalized Magnetization
Temperature (K)
dM / dT

Figure 5

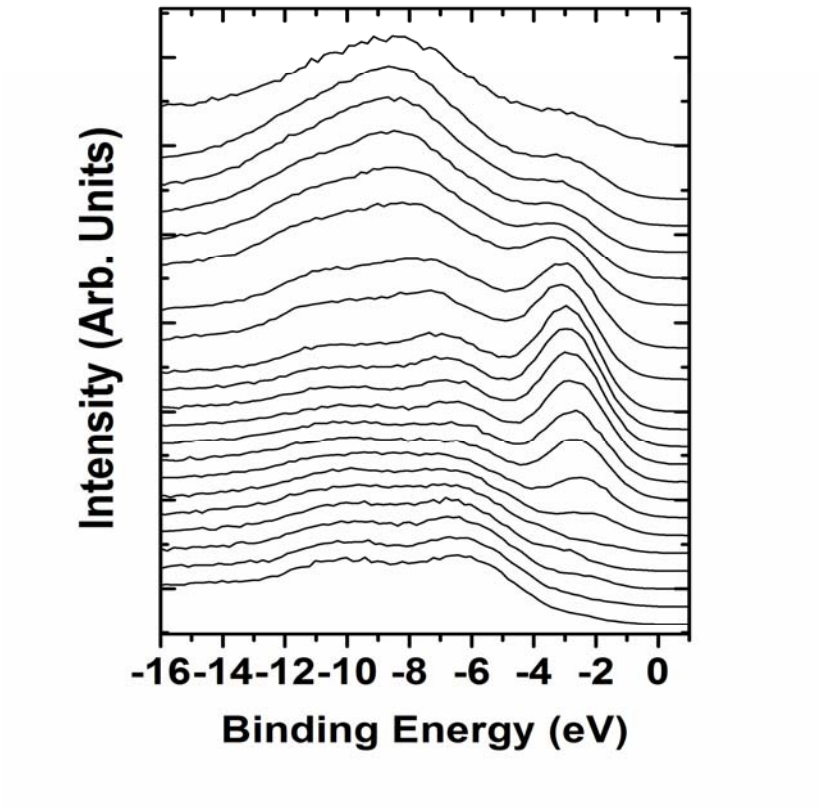

Figure 6

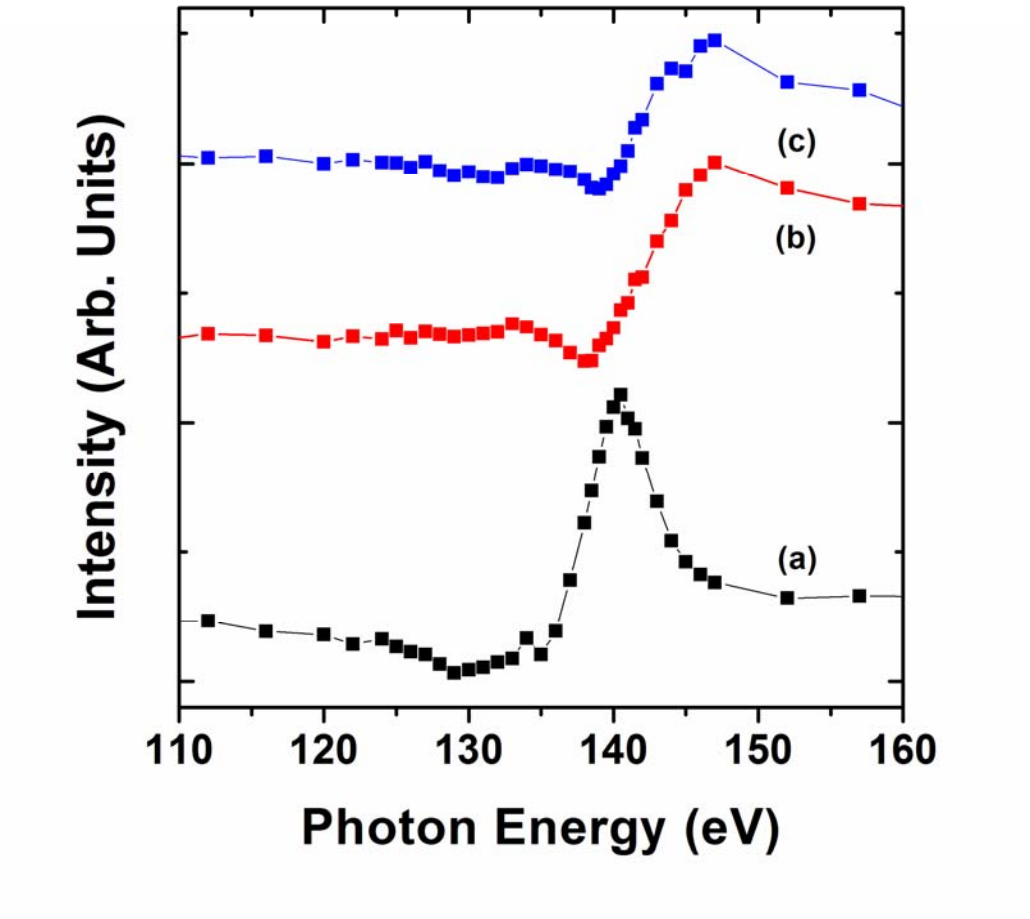
Intensity (Arb. Units)
(c)
(b)
(a)
110
120
130
140
150
160
Photon Energy (eV)